

Two-Coordinate, Quasi-Two-Coordinate, and Distorted Three Coordinate, T-Shaped Chromium(II) Amido Complexes: Unusual Effects of Coordination Geometry on the Lowering of Ground State Magnetic Moments

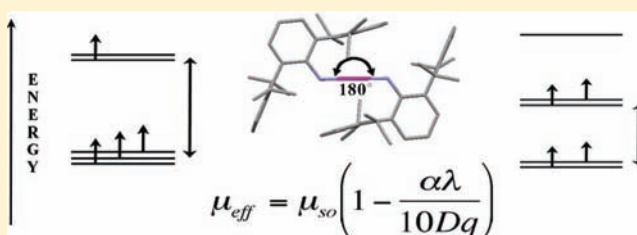
Jessica N. Boynton,[†] W. Alexander Merrill,[†] William M. Reiff,[‡] James C. Fettinger,[†] and Philip P. Power^{*†}

[†]Department of Chemistry, University of California, Davis, One Shields Avenue, Davis, California 95616, United States

[‡]Department of Chemistry and Chemical Biology, Northeastern University, Boston, Massachusetts 02115, United States

S Supporting Information

ABSTRACT: The synthesis and characterization of the mononuclear chromium(II) terphenyl substituted primary amido-complexes $\text{Cr}\{\text{N}(\text{H})\text{Ar}^{\text{Pr}_6}\}_2$ ($\text{Ar}^{\text{Pr}_6} = \text{C}_6\text{H}_3-2,6-(\text{C}_6\text{H}_2-2,4,6-\text{iPr}_3)_2$ (**1**), $\text{Cr}\{\text{N}(\text{H})\text{Ar}^{\text{Pr}_4}\}_2$ ($\text{Ar}^{\text{Pr}_4} = \text{C}_6\text{H}_3-2,6-(\text{C}_6\text{H}_3-2,6-\text{iPr}_2)_2$ (**2**), $\text{Cr}\{\text{N}(\text{H})\text{Ar}^{\text{Me}_6}\}_2$ ($\text{Ar}^{\text{Me}_6} = \text{C}_6\text{H}_3-2,6-(\text{C}_6\text{H}_2-2,4,6-\text{Me}_3)_2$ (**4**), and the Lewis base adduct $\text{Cr}\{\text{N}(\text{H})\text{Ar}^{\text{Me}_6}\}_2(\text{THF})$ (**3**) are described. Reaction of the terphenyl primary amido lithium derivatives $\text{Li}\{\text{N}(\text{H})\text{Ar}^{\text{Pr}_6}\}$ and $\text{Li}\{\text{N}(\text{H})\text{Ar}^{\text{Pr}_4}\}$ with $\text{CrCl}_2(\text{THF})_2$ in a 2:1 ratio afforded complexes **1** and **2**, which are extremely rare examples of two coordinate chromium and the first stable chromium amides to have linear coordinated high-spin Cr^{2+} . The reaction of the less crowded terphenyl primary amido lithium salt $\text{Li}\{\text{N}(\text{H})\text{Ar}^{\text{Me}_6}\}$ with $\text{CrCl}_2(\text{THF})_2$ gave the tetrahydrofuran (THF) complex **3**, which has a distorted T-shaped metal coordination. Desolvation of **3** at about 70 °C gave **4** which has a formally two-coordinate chromous ion with a very strongly bent core geometry ($\text{N}-\text{Cr}-\text{N} = 121.49(13)^\circ$) with secondary $\text{Cr}-\text{C}(\text{aryl ring})$ interactions of 2.338(4) Å to the ligand. Magnetometry studies showed that the two linear chromium species **1** and **2** have ambient temperature magnetic moments of about 4.20 μ_{B} and 4.33 μ_{B} which are lower than the spin-only value of 4.90 μ_{B} typically observed for six coordinate Cr^{2+} . The bent complex **4** has a similar room temperature magnetic moment of about 4.36 μ_{B} . These studies suggest that the two-coordinate chromium complexes have significant spin-orbit coupling effects which lead to moments lower than the spin only value of 4.90 μ_{B} because λ (the spin orbit coupling parameter) is positive. The three-coordinated complex **3** had a magnetic moment of 3.79 μ_{B} .



INTRODUCTION

Strictly linear coordination is known only for a small minority of two-coordinate open shell (d^1-d^9) transition metal complexes in the solid state.^{1,2} Bending of their coordination geometry is generally favored because of (a) ionic intramolecular interactions between the metal ion and electron density at regions of the ligand other than the primary coordination site, (b) packing forces in the crystal structure, or (c) electronic or hybridization effects. However, the use of highly sterically demanding ligands is proving effective for the imposition of rigorously linear coordination in two-coordinate first row transition metal complexes.¹⁻⁷ Ligands based on terphenyl groups are particularly useful because they can be readily functionalized, thereby allowing for the comparison of complexes with electronically similar but sterically different ligands.³

Recent investigations of the magnetic properties of two-coordinate high-spin iron(II) amido complexes show that bending their coordination geometries has a drastic effect on the ground state magnetic moments. In rigorously linear coordination the, d^6 Fe^{2+} ions exhibit essentially free ion magnetic behavior and unprecedentedly large internal hyperfine fields in nuclear gamma resonance spectra because first order orbital

angular momentum remains essentially unquenched since ligation occurs solely on the z -axis.^{4,6,7} Thus, there is a doubly degenerate orbital ground state, which is associated with the unequally occupied degenerate ($d_{x^2-y^2}$, d_{xy})³ orbital configuration of high-spin d^6 . Alternatively, one can say that this set of d orbitals and configuration is nonbonding with respect to the axial σ bonding ligands so that the in plane electron circulation is unfettered and the associated orbital angular momentum is unquenched.^{4,6-8} Upon bending the coordination geometry, however, this degeneracy is expected to be lifted which results in the loss of the first order angular momentum contribution.^{4,6-8} In the bis(amido) iron(II) complexes $\text{Fe}\{\text{N}(\text{H})\text{Ar}^{\text{Pr}_6}\}_2$ and $\text{Fe}\{\text{N}(\text{H})\text{Ar}^{\text{Me}_6}\}_2$, the linear $\text{Fe}\{\text{N}(\text{H})\text{Ar}^{\text{Pr}_6}\}_2$ displayed a much higher magnetic moment (7–7.5 μ_{B}) than the bent species $\text{Fe}\{\text{N}(\text{H})\text{Ar}^{\text{Me}_6}\}_2$ (5.25–5.8 μ_{B}).⁴ Parallel investigations of the analogous Mn^{2+} amides show that their magnetic moments correspond to spin-only values as expected for their high-spin d^5 orbitally nondegenerate (${}^6\text{A}$ or ${}^6\Sigma_g^+$) ground states⁵ whether in bent or linear geometry.⁵

Received: December 15, 2011

Published: February 22, 2012

In contrast to the iron and manganese amides, monomeric two-coordinate chromium(II) amides are almost wholly unknown (likely the result of the extreme instability owing to ready oxidation and of course coordinative unsaturation) and are confined to two borylamide derivatives $\text{Cr}\{\text{N}(\text{Ph})\text{BMes}_2\}_2$ ^{9a} and $\text{Cr}\{\text{N}(\text{Mes})\text{BMes}_2\}_2$ ^{9b} which exhibit strongly bent geometries ($\text{N}-\text{Cr}-\text{N} = 110.8(1)$ and $112.3(3)^\circ$) as well as close interactions (2.32–2.41 Å) with ipso carbons of ligand aromatic substituents.⁹ Other well-characterized Cr(II) amides are either dimerized or complexed with Lewis bases as in $\text{Cr}\{\text{N}(\text{SiMe}_3)_2\}_2(\text{THF})_2$ ¹⁰ or the dimeric species $\{\text{Cr}(\text{NPr}_2)_2\}_2$ ¹¹, $\{\text{Cr}(\text{NPh}_2)_2\}_2$ ¹², $\{\text{Cr}(\text{NCy}_2)_2\}_2$ ¹² and $(\text{Cr}\{\text{N}(\text{1-Ad})\text{C}_6\text{H}_3\text{-3,5-Me}_2\}_2)_2$ (Cy = cyclohexyl, 1-Ad = 1-adamantyl).¹³ The magnetic moments of the mononuclear complexes $\text{Cr}\{\text{N}(\text{Ph})\text{BMes}_2\}_2$ ^{9a}, $\text{Cr}\{\text{N}(\text{Mes})\text{BMes}_2\}_2$ ^{9b} and $\text{Cr}\{\text{N}(\text{SiMe}_3)_2\}_2(\text{THF})_2$ ¹⁰ were reported to have μ_{eff} values 4.91, 4.92, and 4.93 μ_{B} by the Evans' method. In contrast, the moments for the amido dimers were studied as polycrystalline solids over a range of temperatures using a Faraday balance. These were found to have μ_{eff} values varying from 2.30–2.67 μ_{B} , which were interpreted in terms of antiferromagnetic interactions between two low-spin three-coordinate Cr^{2+} ions. The variety of magnetic behavior suggests that further investigation of the magnetic properties of low coordinate chromium complexes is warranted. We now describe the synthesis, characterization, and magnetic properties of four mononuclear Cr(II) amides. These are two derivatives of the very bulky $\text{N}(\text{H})\text{Ar}^{\text{Pr}_6}$ and $\text{N}(\text{H})\text{Ar}^{\text{Pr}_4}$ primary amido ligands which possess very rare linear coordination for chromium. In contrast, strongly bent metal coordination is observed in the less crowded $\text{Cr}\{\text{N}(\text{H})\text{Ar}^{\text{Me}_6}\}_2$ which in turn readily complexes with tetrahydrofuran (THF) to give the three coordinate $\text{Cr}\{\text{N}(\text{H})\text{Ar}^{\text{Me}_6}\}_2(\text{THF})$.

EXPERIMENTAL SECTION

General Procedures. All manipulations were carried out by using modified Schlenk line techniques under a dinitrogen atmosphere or in a Vacuum Atmospheres HE-43 drybox. All of the solvents were first dried by the method of Grubbs et al. and then stored over potassium.¹⁴ All physical measurements were obtained under strictly anaerobic and anhydrous conditions. IR spectra were recorded as Nujol mulls between KBr plates on a Bruker Alpha spectrophotometer. UV–visible spectra were recorded as dilute hexane solutions in 3.5 mL quartz cuvettes using a HP 8452 diode array spectrophotometer. Melting points were determined on a Meltemp II apparatus using glass capillaries sealed with vacuum grease, and are uncorrected. Unless otherwise stated, all materials were obtained from commercial sources and used as received. $\text{CrCl}_2(\text{THF})_2$,¹⁵ $\text{H}_2\text{NAr}^{\text{Me}_6}$,¹⁶ $\text{LiN}(\text{H})\text{Ar}^{\text{Pr}_6}$,¹⁷ and $\text{LiN}(\text{H})\text{Ar}^{\text{Pr}_4}$ ¹⁸ were prepared according to literature procedures.

$\text{Cr}\{\text{N}(\text{H})\text{Ar}^{\text{Pr}_6}\}_2$ (**1**). To a solution of $\text{Ar}^{\text{Pr}_6}\text{NH}_2$ (1.0 g, 2 mmol) in about 30 mL of hexane was added LiBu^n (2.5 M in C_6H_{14}) (0.9 mL, 2.2 mmol) at about -78°C using a dry/acetone bath. After stirring for 24 h, the pale yellow solution was added dropwise to a stirred suspension of $\text{CrCl}_2(\text{THF})_2$ (0.269 g, 1 mmol) in about 30 mL of hexane at about -78°C . The mixture was stirred for 3 days at room temperature, by which time the solution had become orange and a white precipitate had formed. The precipitate was allowed to settle and after careful decanting by cannula, the orange solution was concentrated to about 10 mL, which, upon storage for 1 day at -18°C , afforded X-ray quality bright orange highly air-sensitive crystals of **1**. Exposure to air immediately led to a blue solution. Yield 0.392 g (18%), mp 185–189 $^\circ\text{C}$. Calcd. for $\text{C}_{72}\text{H}_{100}\text{N}_2\text{Cr}$: C, 82.71; H, 9.64; N, 2.68. Found: C, 82.01; H, 9.21; N, 2.54. UV–vis, nm (ϵ , $\text{M}^{-1}\text{cm}^{-1}$), 342 (5100) and 410 (1300). IR in Nujol mull (cm^{-1}) in KBr: $\nu_{\text{N-H}}$ 3350 (w).

$\text{Cr}\{\text{N}(\text{H})\text{Ar}^{\text{Pr}_4}\}_2$ (**2**). To a solution of $\text{Ar}^{\text{Pr}_4}\text{NH}_2$ (2.2 g, 5.3 mmol) in about 30 mL of hexane was added LiBu^n (2.5 M in C_6H_{14}) (2 mL, 6 mmol) at about -78°C . After stirring for 24 h, the pale yellow

solution was added dropwise to a stirred suspension of $\text{CrCl}_2(\text{THF})_2$ (0.713 g, 2.65 mmol) in about 30 mL of hexane cooled in a dry ice/acetone bath. The mixture was stirred for 3 days at room temperature, by which time the solution had become a dull orange/red color and a white precipitate had formed. This was allowed to settle and was separated by careful decanting of the supernatant solution by cannula. The resultant red/orange solution was concentrated to about 10 mL, which, after storage for 1 day at -18°C , afforded X-ray quality air-sensitive red crystals of **2**. Exposure to air led to a blue solution. Yield 0.267 g (12%), mp 288–292 $^\circ\text{C}$. Calcd. for $\text{C}_{60}\text{H}_{96}\text{N}_2\text{Cr}$: C, 82.15; H, 8.73; N, 3.19. Found: C, 81.7; H, 8.77; N, 3.02. UV–vis, nm (ϵ , $\text{M}^{-1}\text{cm}^{-1}$), 340 (3500) and 402 (900). IR in Nujol mull (cm^{-1}) in KBr: $\nu_{\text{N-H}}$ 3354 (w).

$\text{Cr}\{\text{N}(\text{H})\text{Ar}^{\text{Me}_6}\}_2(\text{THF})$ (**3**). To a solution of $\text{Ar}^{\text{Me}_6}\text{NH}_2$ (1.0 g, 3 mmol) in about 30 mL of diethyl ether was added LiBu^n (2.5 M in C_6H_{14}) (1.3 mL, 3.3 mmol) at about -78°C . After stirring for 24 h, the pale yellow solution was added dropwise to a stirred suspension of $\text{CrCl}_2(\text{THF})_2$ (0.403 g, 1.5 mmol) in about 30 mL of diethyl ether cooled to about -78°C in a dry ice/acetone bath. Upon addition, an immediate change to a green colored suspension was observed. The mixture was stirred for 4 days at room temperature, by which time it had become a brown/orange color and a white precipitate had formed. The volatile materials were removed under reduced pressure and hexane (ca. 50 mL) was added, which resulted in a bright orange colored mixture. The precipitate was allowed to settle and after careful decanting by cannula, the dark brown/orange supernatant liquid was concentrated to about 10 mL. Storage for 1 week at -18°C , afforded X-ray quality dichroic orange/green crystals of **3**. Exposure to air led to a blue-black solution. Yield 0.064 g (5.5%), mp 199–206 $^\circ\text{C}$, decomposition at 170 $^\circ\text{C}$. UV–vis, nm (ϵ , $\text{M}^{-1}\text{cm}^{-1}$), 334 (3600) and 402 (1100). IR in Nujol mull (cm^{-1}) in KBr: $\nu_{\text{N-H}}$ 3359 (w).

$\text{Cr}\{\text{N}(\text{H})\text{Ar}^{\text{Me}_6}\}_2$ (**4**). To a solution of $\text{Ar}^{\text{Me}_6}\text{NH}_2$ (1.0 g, 3 mmol) in about 30 mL of diethyl ether cooled to about -78°C was added LiBu^n (2.5 M in C_6H_{14}) (1.3 mL, 3.3 mmol). After stirring for 24 h, the pale yellow solution was added dropwise to a stirred suspension of $\text{CrCl}_2(\text{THF})_2$ (0.401 g, 1.5 mmol) in about 30 mL of diethyl ether cooled to about -78°C . Upon addition, an immediate color change to green was observed. The mixture was stirred for 4 days at room temperature, by which time the solution had become a brown/orange color and a white precipitate had formed. Diethyl ether solvent was removed under reduced pressure and the residue was extracted with three 20 mL aliquots of hot hexane to give a dark orange colored solution. The precipitate was allowed to settle and after careful decanting by cannula, the dark brown/orange solution was concentrated to about 10 mL. Storage for 1 week at -18°C , afforded X-ray quality dark orange air-sensitive crystals of **4**. Exposure to air led to a blue-black solution. Yield 0.079 g (7.4%), mp 199–206 $^\circ\text{C}$. Calcd. for $\text{C}_{48}\text{H}_{52}\text{N}_2\text{Cr}$: C, 81.32; H, 7.39; N, 3.95. Found: C, 81.67; H, 7.58; N, 3.62. UV–vis, nm (ϵ , $\text{M}^{-1}\text{cm}^{-1}$), 336 (1100) and 398 (300). IR in Nujol mull (cm^{-1}) in KBr: $\nu_{\text{N-H}}$ 3359 (w).

X-ray Crystallography. Deep orange-red X-ray quality crystals of **1–4** were obtained from concentrated hexane solutions after storage at -18°C for 2 days. Suitable crystals were selected and covered with a layer of hydrocarbon oil under a rapid flow of dinitrogen. They were mounted on a glass fiber attached to a copper pin and placed in a cold N_2 stream on a diffractometer. X-ray data for **1** and **2** were collected at 90(2) K with 0.71073 Å Mo $\text{K}\alpha$ radiation using a Bruker SMART Apex II diffractometer. Data for **3** and **4** were collected at 90(2) K with 1.5418 Å Cu $\text{K}\alpha_1$ radiation with a Bruker DUO diffractometer in conjunction with a CCD detector.¹⁹ The collected reflections were corrected for Lorentz and polarization effects and for absorption by use of Blessing's method as incorporated into the program SADABS.²⁰ The structures were solved by direct methods and refined with the SHELXTL v.6.1 software package.²¹ Refinement was by full-matrix least-squares procedures with all carbon-bound hydrogen atoms included in calculated positions and treated as riding atoms. N-bound hydrogens were located directly from the Fourier difference map. A summary of crystallographic and data collection parameters for **1–4** is given in Table 1.

Table 1. Selected Crystallographic and Data Collection Parameters for the Complexes 1–4

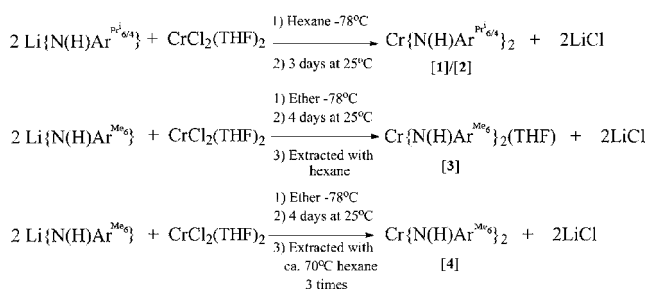
	Cr{N(H)Ar ^{Prⁱ} } ₂ (1)	Cr{N(H)Ar ^{Prⁱ} } ₂ (2)	Cr{N(H)Ar ^{Me^e} } ₂ (THF) (3)	Cr{N(H)Ar ^{Me^e} } ₂ (4)
formula	C ₇₂ H ₁₀₀ N ₂ Cr	C ₆₀ H ₇₆ N ₂ Cr	C ₅₂ H ₆₀ N ₂ O ₂ Cr	C ₄₈ H ₅₂ N ₂ Cr
Fw, g/mol	1045.54	877.23	781.02	708.92
color, habit	orange, rod	red, block	dichroic, block	dark orange, block
crystal system	triclinic	monoclinic	monoclinic	triclinic
space group	<i>P</i> $\bar{1}$	<i>P</i> 2 ₁ / <i>n</i>	<i>P</i> 2 ₁ / <i>c</i>	<i>P</i> $\bar{1}$
<i>a</i> , Å	10.341(2)	10.7222(3)	10.520(2)	13.1525(5)
<i>b</i> , Å	11.393(2)	20.3204(6)	16.081(2)	17.6782(8)
<i>c</i> , Å	14.585(3)	11.2743(3)	25.496(4)	18.5516(7)
α , deg	70.389(3)	90	90	77.851(3)
β , deg	81.988(3)	90.531(1)	90.413(2)	82.704(2)
γ , deg	80.301(3)	90	90	86.023(2)
<i>V</i> , Å ³	1589.0(6)	2456.33(12)	4313.0(11)	4178.7(3)
<i>Z</i>	1	2	4	2
crystal dims, mm	0.41 × 0.34 × 0.29	0.199 × 0.193 × 0.243	0.098 × 0.366 × 0.645	0.148 × 0.246 × 0.455
<i>T</i> , K	90(2)	90(2)	90(2)	90(2)
<i>d</i> _{calc} , g/cm ³	1.093	1.186	1.203	1.195
abs. coefficient μ , mm ⁻¹	0.221	0.273	0.305	0.314
θ range, deg	1.49–27.50	2.61–27.50	1.94–27.48	2.45–68.25
obs reflections [<i>I</i> > 2 σ (<i>I</i>)]	6140	4782	8352	12198
data/restraints/parameters	7278/0/356	5639/0/438	9881/21/534	14018/25/105
<i>R</i> ₁ , observed reflections	0.064	0.0366	0.0448	0.0935
<i>wR</i> ₂ , all	0.1932	0.0462	0.0519	0.1039

Magnetic Measurements. Polycrystalline samples of complexes 1–4 were sealed under vacuum in 3 mm diameter quartz tubes for magnetic studies. The samples' magnetizations were measured using a Quantum Design MPMSXL7 Superconducting Quantum Interference Device (SQUID). In each case the sample was zero-field cooled to 4 K. The magnetization was measured upon warming to 380 K in an applied field of 0.01 T (100 Oe). Diamagnetic corrections of -766×10^{-6} , -624×10^{-6} , -535×10^{-6} , and -482×10^{-6} emu/mol, obtained from tables of Pascal's constants,²² were applied to the measured molar magnetic susceptibilities of complexes 1–4, respectively.

RESULTS AND DISCUSSION

Synthesis. Compounds 1–4 were synthesized via salt metathesis routes as shown in Scheme 1. While the synthetic

Scheme 1. Synthetic Routes to 1–4



routes appear straightforward, they required considerable investigation of the reaction conditions to obtain reliable product yields. A variety of solvents such as diethyl ether, tetrahydrofuran, toluene, and so forth, as well as reaction temperatures, were tested for these reactions. It was found that a synthetic procedure involving the slow addition of lithium primary aryl amide Li{N(H)Ar} to a hexane (1 and 2) or diethyl ether (3 and 4) suspension of the metal halide-tetrahydrofuran complex cooled to about -78°C afforded the most consistent results. The initial green color of the reaction

mixtures slowly deepened to orange upon warming to room temperature. Stirring had to be continued for extended periods (ca. 2–4 days) to obtain significant yields of the products 1–4, and crystals were grown from the reaction solution (after separation for the LiCl precipitate) by concentration and cooling to about -18°C of the hexane extracts of the dry reaction mixtures. Solutions of 1–4 were highly sensitive such that filtration through Celite padded glass frit invariably resulted in significant decomposition even when extreme precautions were taken to exclude air and moisture. We found that separation of the solutions from the precipitate by decanting afforded the products 1–4 in relatively low but reproducible yield.

The synthesis of 1–4 differs from the approach used for the iron complexes Fe{N(H)Ar^{Prⁱ}}₂ and Fe{N(H)Ar^{Me^e}}₂ which were obtained by transamination involving the treatment of Fe{N(SiMe₃)₂}₂²³ with 2 equiv of the respective primary amines. This approach was used because the alkali metal salt elimination route analogous to that used for 1–4 (Scheme 1) proved unsatisfactory owing to sluggish reactions and the formation of anionic products. In contrast, the greater solubility of CrCl₂(THF)₂ permitted reactions to occur, albeit slowly, to afford 1–4 in low but acceptable yields. The reasons for the low-yields in these reactions are unclear at present. However, the slow rate of reaction, which probably involves an unfavorable nucleophilic attack on the square planar geometry CrCl₂(THF)₂ complex, together with the possible formation of salt-like products, may be factors in reducing the yields.

Structures. The structures of 1 and 2 are shown below in Figures 1 and 2. Selected bond lengths and angles are presented in Table 2 along with data from their manganese⁵ and iron⁴ analogues. The structure of the bent geometry bis(amido) complex 4 is shown in Figure 3. Selected structural data for 4 and its manganese and iron analogues are given in Table 3.

Complexes 1 and 2 are the first reported examples of linear coordinated amido chromium species. Linear coordination for chromium is very rare and has precedent only in the related Cr²⁺ thiolato complex Cr(SAr^{Prⁱ})₂.²⁴ The ipso carbons of the

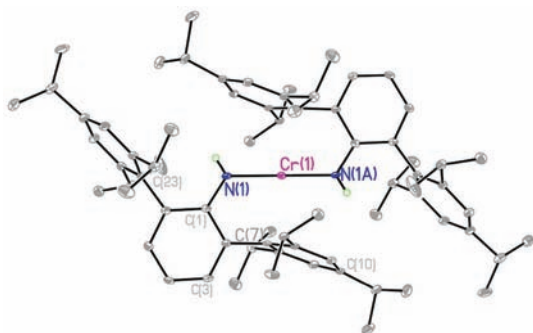


Figure 1. X-ray crystal structure of linearly coordinated $\text{Cr}\{\text{N}(\text{H})\text{Ar}^{\text{Pr}^i}\}_2$ (**1**). (Non-nitrogen H atoms are not shown for clarity, thermal ellipsoids are shown at 30% probability.) Select bond distances and angles are given in Table 2.

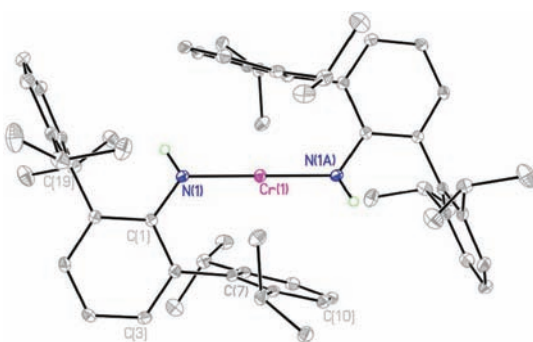


Figure 2. X-ray crystal structure of linearly coordinated $\text{Cr}\{\text{N}(\text{H})\text{Ar}^{\text{Pr}^i}\}_2$ (**2**). (Non-nitrogen H atoms are not shown for clarity, thermal ellipsoids are shown at 30% probability.) Select bond distances and angles are listed in Table 2.

Table 2. Selected Interatomic Distances (Å) and Angles (deg) for the Linear Complexes 1 and 2 and the Mn⁵ and Fe⁴ Derivatives of N(H)Ar^{Prⁱ}.

	$\text{Cr}\{\text{N}(\text{H})\text{Ar}^{\text{Pr}^i}\}_2$ [1]	$\text{Cr}\{\text{N}(\text{H})\text{Ar}^{\text{Pr}^i}\}_2$ [2]	$\text{Mn}\{\text{N}(\text{H})\text{Ar}^{\text{Pr}^i}\}_2$	$\text{Fe}\{\text{N}(\text{H})\text{Ar}^{\text{Pr}^i}\}_2$
M–N (Å)	1.9966(14)	1.9775(12)	1.952(2)	1.907(14)
M---(C7,7A) (Å)	2.481(2)	2.630	2.73	2.79
N–M–N (deg)	180.0	180.0	176.09(12)	180.0
M–N–H (deg)	121.3(18)	121.3(13)		117.5(16)
C–N–M (deg)	123.33(11)	125.70(9)		130.06(11)

central aryl rings of the terphenyl group, the nitrogens, the hydrogens on the two nitrogens, and chromium form a plane with the terphenyls in a trans-fashion resulting in local C_{2h} symmetry for the $\text{M}\{\text{N}(\text{H})\text{C}(\text{ipso})\}_2$ arrays. The key structural data for **1** and **2** and related manganese and iron species are summarized in Table 2. The M–N distances in **1**, 1.9966(14) Å, and **2**, 1.9775(12) Å, are very similar. The bond lengths are significantly longer than those in the corresponding manganese⁵ and iron⁴ complexes consistent with the decreasing size (Cr, 1.22 Å; Mn, 1.19 Å; Fe, 1.16 Å) of the metal radius on proceeding to the right across the d-block.²⁵ They are about 0.1 Å shorter than the 2.09(1) Å Cr–N bond length in $\text{Cr}\{\text{N}(\text{SiMe}_3)_2\}_2(\text{THF})_2$ which has four-coordinate Cr(II) in square planar complexation. However, the bonds are longer than the terminal Cr–N distances of 1.927(3) and 1.942(7) Å

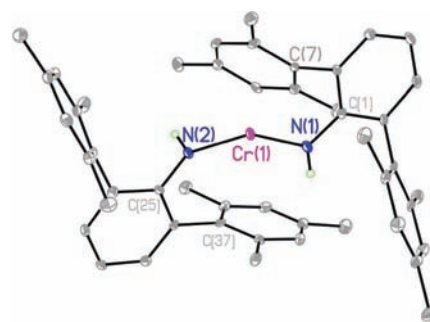


Figure 3. Thermal ellipsoid drawing (30%) of the X-ray crystal structure of nonlinear coordinated $\text{Cr}\{\text{N}(\text{H})\text{Ar}^{\text{Me}_c}\}_2$ (**4**). (Non-nitrogen H atoms are not shown for clarity.) Select bond distances and angles are given in Table 3.

Table 3. Selected Interatomic Distances (Å) and Angles (deg) for the Bent Complex 4 and the Corresponding Mn⁵ and Fe⁴ Derivatives^a

	$\text{Cr}\{\text{N}(\text{H})\text{Ar}^{\text{Me}_c}\}_2$ (4)	$\text{Mn}\{\text{N}(\text{H})\text{Ar}^{\text{Me}_c}\}_2$ ⁵	$\text{Fe}\{\text{N}(\text{H})\text{Ar}^{\text{Me}_c}\}_2$ ⁴
M–N(1) (Å)	1.977(3)	1.976(2)	1.909(3)
M–N(2) (Å)	1.943(3)	1.982(3)	1.913(3)
M---(<i>i</i> -MesC) (Å)	2.338(4)	2.63	2.64
N(1)–M–N(2) (deg)	121.49(13)	138.19(9)	141.94(16)
M–N(1)–H(1) (deg)	119.1		116
M–N(2)–H(2) (deg)	111.7		114
C(1)–N(1)–M (deg)	121.8(2)		128.5(3)
C(25)–N(2)–M (deg)	136.7(2)		127.2(3)

^aThe average distance of M---(*i*-MesC) interactions are also given.

in the dimers $\text{R}_2\text{N}(\text{Cr}(\mu\text{-NR}_2)_2\text{CrNR}_2)$ (R = Prⁱ and Cy)¹² which have three-coordinate Cr(II).

There are also relatively close interactions between the metal and ipso carbon from one of the flanking aryl rings of the terphenyl ligand of 2.48 Å for complex **1** and 2.63 Å for complex **2**. These structural data support the view that terphenyl based ligands protect space surrounding the metal primarily via the shielding action of their flanking aryl rings. In this respect, inspection of the structures of **1** and **2** shows that **1** is the more crowded molecule. The presence of para-isopropyl groups on the flanking aryl rings cause the $\text{C}_6\text{H}_2\text{-2,4,6-Pr}^i_3$ ring closest to the chromium to bend away from the metal as indicated by an angle of 19.56° between the C(2)–C(7) bond and the plane of the C(7) ring. This bending is caused by the interaction of the para Prⁱ group and the flanking ring of the opposite Ar^{Prⁱ} ligand. However, the shorter Cr---C interactions in **1** are probably caused by the presence of the para –Prⁱ groups on the flanking aryl rings that cause trans-metallic steric repulsion (i.e., between the para –Prⁱ substituents on the C(23) and C(7A) flanking tri-iso-propyl phenyl rings) which cause the Cr–N–C(ipso) angles to close (cf. Table 2, C–N–M angles = 123.33(11) in **1** and 125.70(9)° in **2** and give a shorter Cr---C approach in **1**.

The structure of the complex $\text{Cr}\{\text{N}(\text{H})\text{Ar}^{\text{Me}_c}\}_2$ (**4**) is shown in Figure 3. Key structural data for this complex as well as data for its manganese and iron congeners are given in Table 3. These show that **4** has a very strongly bent coordination with a N–Cr–N angle of 121.49(13)° which resembles the N–Cr–N angles of 110.8(1)° in the borylamido complexes $\text{Cr}\{\text{N}(\text{Ph})\text{-BMe}_2\}_2$ and 112.3(3)° in $\text{Cr}\{\text{N}(\text{Mes})\text{BMe}_2\}_2$. It is also noteworthy that the degree of bending in **4** is considerably

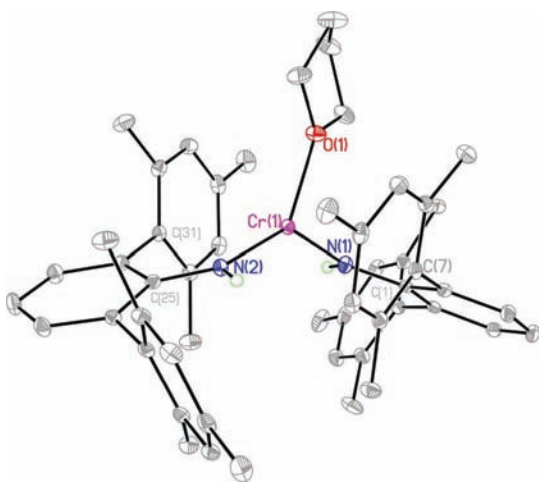


Figure 4. Thermal ellipsoid drawing (30%) of the X-ray crystal structure of the three-coordinated $\text{Cr}\{\text{N}(\text{H})\text{Ar}^{\text{Me}_6}\}_2(\text{THF})$, (**3**). (Non-nitrogen H atoms are not shown for clarity.) Select bond distances and angles are given in Table 4.

Table 4. Selected Interatomic Distances (Å) and Angles (deg) for **3 and the Related Mn^{V} Derivative^a**

	$\text{Cr}\{\text{N}(\text{H})\text{Ar}^{\text{Me}_6}\}_2(\text{THF})$ [3]	$\text{Mn}\{\text{N}(\text{H})\text{Ar}^{\text{Me}_6}\}_2(\text{THF})^{\text{S}}$
M–N(1) (Å)	1.9779(14)	1.986(2)
M–N(2) (Å)	1.9546(14)	1.988(2)
M–O (Å)	2.0682(13)	2.175(2)
M···(<i>i</i> -MesC) (Å)	2.948	2.907
N(1)–M–N(2) (deg)	132.08(6)	143.83(5)
N(1)–M–O(1) (deg)	134.36(5)	117.10(7)
N(2)–M–O(1) (deg)	93.44(6)	99.05(7)

^aThe average distance of M···(*i*-MesC) interactions are given.

greater (by ca. 17°) than that in its manganese analogue. The Cr–N distances in **4**, 1.977(3) and 1.943(3) Å, are slightly shorter than those in **1** and **2**. Thus the data in Tables 2 and 3, show that as the bulk of the ligand decreases, so do the Cr–N bond lengths, supporting the view that the steric crowding causes the slight lengthening of the bond in more hindered complexes **1** and **2**. The structure **4** also has the closest interaction between the metal and ipso carbon from one of the flanking aryl rings of the terphenyl ligand at only 2.338(4) Å.

The THF complex **3** shown in Figure 4 is a relatively rare example of a monomeric three-coordinate chromium(II) complex,^{26–28} and is analogous to the manganese Lewis base adduct $\text{Mn}\{\text{N}(\text{H})\text{Ar}^{\text{Me}_6}\}_2(\text{THF})$.⁵ The interaction between the metal and ipso carbon from one of the flanking aryl rings of the terphenyl ligand is prevented by the coordination to the THF (Cr–O = 2.338(4) Å) and a very long distance of 2.948 Å to the closest flanking aryl carbon is observed. M–N distances, 1.9779(14) and 1.9546(14) Å, are only slightly lengthened despite the higher metal coordination number.

The most interesting feature of the structure of **3** is the highly distorted metal coordination. Although the metal coordination is planar, the two O–Cr–N angles, 134.36(5) and 93.44(6)°, differ by more than 40° (cf. an 18° difference in its manganese analogue). There is growing evidence that the gross irregularities in the interligand angles in three-coordinate Cr(II) complexes is a preferred coordination mode. An analysis by Baik, Mindiola, and co-workers of the structural distortions in several β -diketiminato Cr(II) derivatives, combined with density functional theory

(DFT) calculations, led them to the conclusion that σ -donor coligands favor T-coordination whereas π -donor ligands prefer Y-coordination.²⁷ To classify the geometries they introduced a “*T*” parameter which was defined as the difference between the two N–Cr–X angles divided by 90°. The *T* values can range from 0 (perfectly Y-shaped) to 1 (a perfect T-shape). Because of the large size of the β -diketiminato ligand that was employed, an ideal *T* value of 1 was deemed unlikely. However, the geometry can be regarded as distorted T-shaped when the *T* values become significantly larger than 0, and they chose a value that was larger than 0.1 as the characteristic criterion for a distorted T-shaped geometry. The largest *T* value they observed for their β -diketiminato derivatives was 0.447 for a σ -donating coligand. It can be seen from the data provided for **3** in Table 5, that **3** has a very similar

Table 5. Comparison of *T*-Values of Selected Three-Coordinate Cr(II) Complexes

	$\text{Cr}\{\text{N}(\text{H})\text{Ar}^{\text{Me}_6}\}_2(\text{THF})$ (3) ^a	$\text{Cr}\{(\mu\text{-NH}_2)\text{CrAr}^{\text{Pr}^t}\}_2$ ^{b,28}	$(\text{THF})\text{LiClCr}(\text{OCBu}^t_3)_2$ ^{c,26}
L–Cr–X	134.36(5)	110.11(7)	110.9(1)
L–Cr–X	93.44(6)	86.21(8)	91.1(1)
difference	40.92	23.90	19.8
<i>T</i> value ^d	0.455	0.266	0.22

^aL = N(H)Ar^{Me₆}, X = O. ^bL = NH₂, X = Ar^{Pr^t}. ^cL = OCBu^t₃, X = Cl. ^d*T* = angular difference divided by 90°.

three-coordinate *T* value of 0.455. Table 5 also includes structural data for two Cr(II) complexes with all monodentate ligands which meet the *T* value for distorted T-shaped geometry. This is very much in agreement with the σ -donor character of the THF ligand. The remaining two complexes, $\text{Cr}\{(\mu\text{-NH}_2)\text{CrAr}^{\text{Pr}^t}\}_2$ ²⁸ and $(\text{THF})\text{LiClCr}(\text{OCBu}^t_3)_2$ ²⁶ also feature *T* values well above the 0.1 criterion for distorted T-shaped geometry. It is of course possible to argue that our analysis of the geometry of the three complexes is unjustified since the X–Cr–X angles are much wider than the about 90° bite angle of the β -diketiminates. Nonetheless, the essential message is that the complexes involved all have very severe distortions from regular trigonal geometries.

Electronic Spectroscopy. The UV–visible absorption spectra of the intensely colored complexes **1–4** in dilute hexane solution revealed moderately intense electronic transitions for the series of the linear complexes. UV–vis absorption peaks (λ_{max} , nm (ϵ , M^{−1} cm^{−1})) were observed at 342 (5100) and 410 (1300) for linear complex **1**. The other linear complex **2** displayed two similar absorptions at 340 (3500) and 402 (900). The three-coordinate complex **3** also displayed two absorption maxima at 334 (3600) and 402 (1100). The bent two-coordinate complex **4** had absorption maxima at 336 (1100) and 398 (300). Crystalline samples and solutions of the linear compound **1** were intensely orange while those of **2** were a darker red/orange. Both nonlinear chromium compounds **3** and **4** had a darker orange/brown color. The observation of similar spectra for **1–4** suggest that their structures are broadly similar in solution. If it is assumed that the ⁵D₀ ground state of Cr²⁺ has approximately linear coordination it will be split into ⁵Σ_g⁺, ⁵Π_g, and ⁵Δ_g states (for local D_{∞h} symmetry) so that the higher energy (ca. 340 nm) and lower energy transitions at about 400 nm could be assigned to Σ_g⁺ → Δ_g and Σ_g⁺ → Π_g transitions. However, definitive assignments are not possible because of the lack of both comparison data and detailed computational work on the energy states. It is noteworthy that these wavelengths

Table 6. Curie–Weiss Law-Parameters Derived for Complexes 1–4

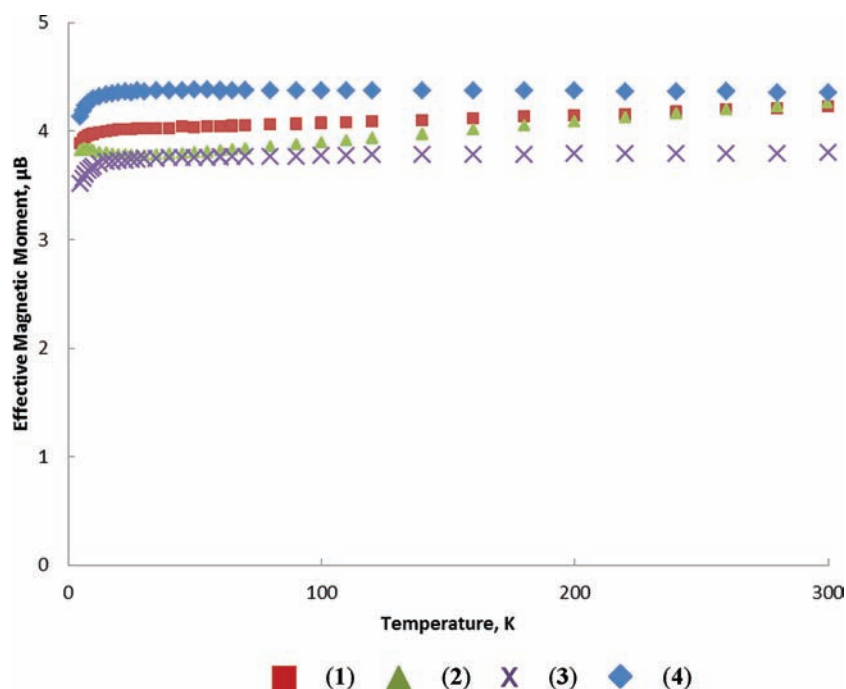
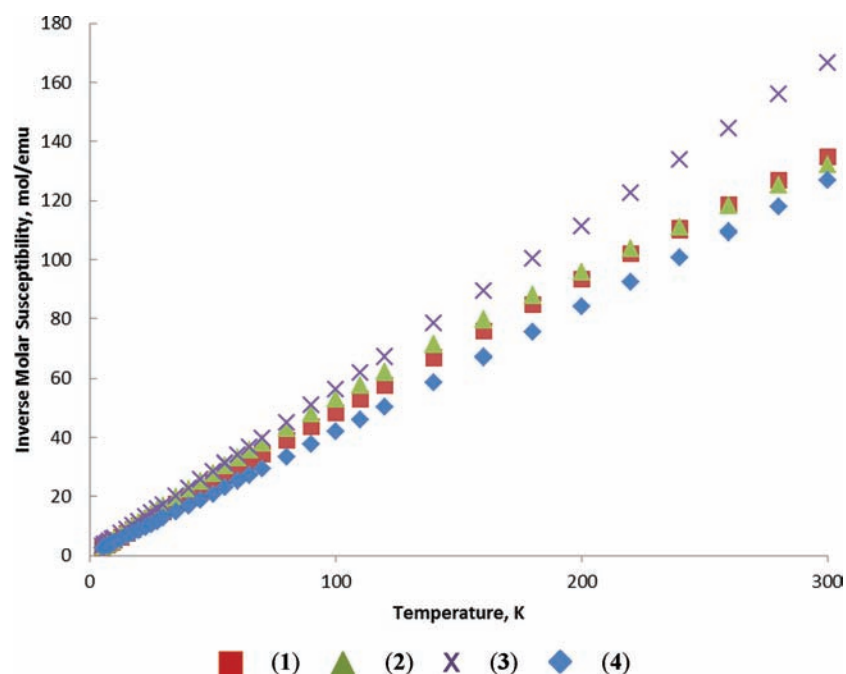
complex	temperature range/K	$C/\text{emu K mol}^{-1}$	$\mu_{\text{eff}}^a \mu_{\beta}$
1	5–300	2.20	4.20
2	5–300	2.34	4.33
3	5–300	1.80	3.79
4	5–300	2.38	4.36

^aThe effective magnetic moment obtained from the Curie constant, C , and uncorrected for any values of H .

when converted to cm^{-1} frequency units become 29,400 and 25,000 cm^{-1} . These values suggest either that the ligand field

splitting is quite large or that the absorptions involve charge transfer. Since the former possibility seems inconsistent with the low coordination number, the latter possibility combined with their broadness suggests they are charge transfer transitions.

DC Magnetometry Measurements. The DC SQUID magnetometry results for complexes 1 through 4 are summarized in Table 6 and Figures 5 and 6. In view of the linearity of the χ^{-1} versus T data for complexes 1, 3, and 4 over the entire temperature range 5 to 300 K, it seems reasonable to assume that these systems more or less conform to a single Curie–Weiss Law while the plot for complex 2 deviates somewhat from linearity. This in turn is likely the result of trace

**Figure 5.** μ_{EFF} versus T plots for complexes 1–4.**Figure 6.** Inverse molar susceptibilities versus T plots for complexes 1–4.

impurity or possibly that **2** undergoes some type of structural transformation or phase change at intermediate temperature. The latter have in fact been observed for other linear systems studied in our laboratory via X-ray crystallography.²⁸

In attempting to account for the uniformly lower than predicted magnetic moments of **1–4**, we note that previous detailed magnetic susceptibility investigations of divalent chromium compounds are almost exclusively concerned with octahedral or six coordinate pseudo-octahedral complexes. As such their effective moments are generally close to the spin-only moment expected ($\sqrt{24}$ or $4.89 \mu_B$) for the high-spin d^4 configuration. These moments are usually discussed in terms of the equation $\mu_{\text{eff}} = \mu_{\text{so}}(1 - \alpha\lambda/10Dq)$, corresponding to a second-order effect of spin-orbit coupling^{29,30} where for the free ion 5D ground term of Cr^{2+} , the spin-orbit coupling parameter λ is $+57 \text{ cm}^{-1}$.³⁰ The J states for this ground term are 0, 1, 2, 3, 4 and span 10λ (using the Landé interval rule) or some 570 cm^{-1} . For $d^4 \alpha = 2$ and $10Dq$ has its usual meaning of the ligand field splitting. The expected decrease in μ_{eff} implied (by the second “negative” term) of the foregoing equation is usually very small, and the observed moments are usually not significantly different from μ_{so} consistent with the orbitally nondegenerate 5B ground state of Cr^{2+} resulting from Jahn–Teller distortion of the degenerate 5E in regular octahedral geometry. Matters change somewhat on going to rigorously linear Cr^{2+} . The ground state is still orbitally nondegenerate and as such cannot exhibit a first order orbital angular momentum contribution to the moment. However, with the smaller overall ligand field expected for two coordination, the decrease in the moment is produced by the negative term in the above equation, and is clearly more apparent in the observed effective moments presented herein. Alternatively, one can say that with fewer ligands and approach to coordinative unsaturation, we are inevitably approaching the free ion ground state manifested in the symbology 5D_0 , that is, $J = L + S = 0$ (complexes **1** and **2** of Table 6). To our knowledge, the present study represents the first, clearly unequivocal, manifestation of this moment decreasing spin-orbit effect because λ is positive for Cr^{2+} and the systems studied are highly coordinatively unsaturated. In view of the structures we have found, this effect does not seem likely to be the result of any antiferromagnetic interactions between the monomeric units of these complexes.

CONCLUSION

Four monomeric, analytically pure chromium(II) amido complexes with somewhat differing coordination geometries at the metal centers have been successfully synthesized and characterized, despite their extreme air sensitivity and chemical reactivity owing to extreme coordinative unsaturation. Species **1** and **2**, with the bulkier terphenyl amido ligands, were shown to have rigorously linear geometry. However, the less bulky ligand $-\text{N}(\text{H})\text{Ar}^{\text{Me}_6}$, permits significantly bent geometry owing to reduced trans-metallic ligand repulsion in the complex **4**. The lowered steric requirement of the $-\text{N}(\text{H})\text{Ar}^{\text{Me}_6}$ ligand also permits coordination of THF to the metal in **3**. Complexes **1** through **4** have no first order orbital angular momentum contribution to their magnetic moments but have magnetic moments clearly less than the spin-only value as a result of spin-orbit coupling and the smaller overall ligand field arising from the low number of ligands. This is an expected but not well-studied property of early transition metals with less than half filled d orbitals, since the positive spin orbit coupling detracts from the magnetic moment rather than enhancing it as in the case of later transition metal

elements. Further studies of these complexes involving EPR, electrochemical and computational techniques are in hand.

ASSOCIATED CONTENT

Supporting Information

CIF files for the X-ray structures of **1–4**. This material is available free of charge via the Internet at <http://pubs.acs.org>.

AUTHOR INFORMATION

Corresponding Author

*E-mail: pppower@ucdavis.edu.

Notes

The authors declare no competing financial interest.

ACKNOWLEDGMENTS

We are grateful to the National Science foundation (CHE-0948417) for financial support and Peter Klavins for assistance in the magnetization measurements.

REFERENCES

- (1) Power, P. P. *Chemtracts–Inorg. Chem.* **1994**, *6*, 181.
- (2) Kays, D. L. *Dalton Trans.* **2011**, *40*, 769.
- (3) Ni, C.; Power, P. P. *Struct. Bonding (Berlin)* **2010**, *136*, 59.
- (4) Merrill, W. A.; Stich, T. A.; Brynda, M.; Yeagle, G. J.; Fetting, J. C.; De Hont, R.; Reiff, W. M.; Schulz, C. E.; Britt, R. D.; Power, P. P. *J. Am. Chem. Soc.* **2009**, *131*, 12693.
- (5) Ni, C.; Rekken, B.; Fetting, J. C.; Long, G. J.; Power, P. P. *J. Chem. Soc., Dalton Trans.* **2009**, 8359.
- (6) (a) Reiff, W. M.; La Pointe, A. M.; Witten, E. H. *J. Am. Chem. Soc.* **2004**, *126*, 10206. The $\text{Fe}\{\text{C}(\text{SiMe}_3)_3\}_2$ complex studied in (a) was originally described in: (b) Viefhaus, T.; Schwartz, W.; Hübler, K.; Locke, K.; Weidlein, J. Z. *Anorg. Allg. Chem.* **2001**, *627*, 715. and (c) LaPointe, A. M. *Inorg. Chim. Acta* **2003**, *345*, 359.
- (7) Reiff, W. M.; Schulz, C. E.; Whangbo, M. H.; Seo, J. I.; Lee, Y. S.; Potratz, G. R.; Spicer, C. W.; Girolami, G. S. *J. Am. Chem. Soc.* **2009**, *131*, 404.
- (8) Drago, R. S. *Physical Methods for Chemists*; Harcourt Brace Jovanovich: New York, 1993; p 484.
- (9) (a) Chen, H.; Bartlett, R. A.; Olmstead, M. M.; Power, P. P.; Shoner, S. C. *J. Am. Chem. Soc.* **1990**, *112*, 1048. (b) Bartlett, R. A.; Chen, H.; Power, P. P. *Angew. Chem., Int. Ed.* **1989**, *28*, 319.
- (10) Bradley, D. C.; Hursthouse, M. B.; Newing, C. W.; Welch, A. J. *J. Chem. Soc., Chem. Commun.* **1972**, 567.
- (11) Edema, J. J. H.; Gambarotta, S.; Spek, A. L. *Inorg. Chem.* **1989**, *28*, 812.
- (12) Edema, J. J. H.; Gambarotta, S.; Meetsma, A.; Spek, A. L.; Smeets, W. J.; Chiang, M. Y. *J. Chem. Soc., Dalton Trans.* **1993**, 789.
- (13) Rupp, K. B. P.; Feghali, K.; Kovacs, I.; Aparna, K.; Gambarotta, S.; Yap, G. P. A.; Bensimon, C. *J. Chem. Soc., Dalton Trans.* **1998**, 1595.
- (14) Pangborn, A. B.; Giardello, M. A.; Grubbs, R. H.; Rosen, R. K.; Timmers, F. J. *Organometallics* **1996**, *15*, 1518.
- (15) Betz, P.; Jolly, P. W.; Kruger, C.; Zakrzewski, U. *Organometallic Chem.* **1991**, *91*, 3520.
- (16) Tilley, T. D.; Gavenonis, J. *Organometallics* **2000**, *21*, 5549.
- (17) Twamley, B.; Hwang, C. S.; Hardman, N. J.; Power, P. P. *J. Organomet. Chem.* **2000**, *609*, 152.
- (18) Ditri, T. B.; Fox, B. J.; Moore, C. E.; Rheingold, A. L.; Figueroa, J. S. *Inorg. Chem.* **2009**, *48*, 8362.
- (19) Hope, H. *Prog. Inorg. Chem.* **1995**, *41*, 1.
- (20) (a) Blessing, R. H. *Acta Crystallogr.* **1995**, *A51*, 33. (b) Sheldrick, G. M. *SADABS, Siemens Area Detector Absorption Correction*; Universität Göttingen: Göttingen, Germany, 2008.
- (21) (a) Sheldrick, G. M. *SHELXTL*, Version 6.1; Bruker AXS Inc.: Madison, WI, 2002. (b) Sheldrick, G. M. *SHELXS97 and SHELXL97*; Universität Göttingen: Göttingen, Germany, 1997.
- (22) Bain, G. A.; Berry, J. F. *J. Chem. Educ.* **2008**, *85*, 532.

- (23) Andersen, R. A.; Faegri, K.; Green, J. C.; Haaland, A.; Lappert, M. F.; Leung, W.-P.; Rypdal, K. *Inorg. Chem.* **1988**, *27*, 1782.
- (24) Nguyen, T.; Panda, A.; Olmstead, M. M.; Richards, A. F.; Stender, M.; Brynda, M.; Power, P. P. *J. Am. Chem. Soc.* **2005**, *127*, 8545.
- (25) Pyykkö, P.; Atsumi, M. *Chem.—Eur. J.* **2009**, *15*, 12770.
- (26) Hvoslef, J.; Hope, H.; Murray, B. D.; Power, P. P. *J. Chem. Soc., Chem. Commun.* **1983**, 1438.
- (27) Fan, H.; Adhikari, D.; Saleh, A. A.; Clark, R. L.; Zuno-Cruz, F.; Cabrera, G. S.; Huffman, J. C.; Pink, M.; Mindiola, D. J.; Baik, M.-H. *J. Am. Chem. Soc.* **2008**, *130*, 17351.
- (28) Ni, C.; Long, G. J.; Grandjean, F.; Power, P. P. *Inorg. Chem.* **2009**, *48*, 11594.
- (29) Figgis, B. N. *Faraday Trans.* **1960**, *56*, 1553.
- (30) Figgis, B. N. *Introduction to Ligand Fields*; Wiley: New York, 1960; p 60 and 265.